Published in: European Journal of Cardio-Thoracic Surgery (2003), vol.24, pp.912-919
Status: Postprint (Author's version)

Effects of increased afterload on left ventricular performance and mechanical efficiency are not baroreflex-mediated

Philippe Kolh, Alexandre Ghuysen, Vincent Tchana-Sato, Vincent D'Orio, Paul Gerard, Philippe Morimont, Raymond Limet, Bernard Lambermont

Haemodynamic Research Center (HemoLiege), University of Liege, Liege, Belgium

Abstract:

Objective: To assess baroreflex intervention during increase in left ventricular afterload, we compared the effects of aortic banding on the intact cardiovascular system and under hexamethonium infusion. **Methods:** Six open-chest pigs, instrumented for measurement of aortic pressure and flow, left ventricular pressure and volume, were studied under pentobarbital-sufentanil anesthesia. Vascular arterial properties were estimated with a four-element windkessel model. Left ventricular contractility was assessed by the slope of end-systolic pressure-volume relationship. **Results:** The effects of aortic banding on mechanical aortic properties were unaffected by autonomic nervous system inhibition. However, increase in peripheral arterial vascular resistance and in heart rate were prevented by hexamethonium. Aortic banding increased left ventricular contractility and stroke work. Left ventricular-arterial coupling remained unchanged, but mechanical efficiency was impaired. These ventricular changes were independent of baroreflex integrity. **Conclusions:** Our results demonstrate that an augmentation in afterload has a composite effect on left ventricular function. Left ventricular performance is increased, as demonstrated by increase in contractility and stroke work, but mechanical efficiency is decreased. These changes are observed independently of baroreflex integrity. Such mechanisms of autoregulation, independent of the autonomic nervous system, are of paramount importance in heart transplant patients.

Keywords: Autonomic nervous system; Baroreflex; Hemodynamics; Left ventricular function

1. Introduction

The organism has several adaptive mechanisms that aim at keeping cardiac output constant when the needs of the body change or when the hemodynamic loading conditions under which the heart must operate are modified. Although in studies of isolated cardiac muscle or chambers removed from the circulation, specific responses to isolated alterations in test conditions can be evaluated, the situation is different in the intact animal because changes in one parameter generally lead to secondary changes in others. Therefore, the response of the in vivo preparation may differ from that of an isolated heart, even though a similar initial perturbation is being investigated.

One example of this problem is how the left ventricle (LV) reacts to an increase in afterload. In an isolated heart preparation, it is possible to fix LV end-diastolic volume and to impose several afterload conditions [1]. However, in the intact organism, any afterload augmentation induces a recruitment of the preload reserve mechanism, such that LV end-diastolic volume secondarily increases [2]. Because a progressive augmentation in myofiber length increases cardiac performance secondary to an heterometric adaptation, the integrated response to increased afterload of an intact organism may indeed differ from the response observed in an isolated heart preparation.

Therefore, the aim of this experimental study was to evaluate, in vivo, the LV response to an afterload augmentation, obtained by means of a proximal aortic banding. In addition, in order to assess the role of baroreflex intervention under these circumstances, we compared the effects of the aortic banding on the intact cardio-vascular system, and when the baroreflex mechanism was inhibited by hexamethonium and atropine infusion.

Chamber properties and energetics were analyzed with the pressure-volume relationship, and LV afterload was assessed using a four-element windkessel model.

2. Methods

2.1. Surgical preparation

Experiments were performed on six healthy pigs of either sex weighing from 20 to 28 kg. All the animals

received humane care in compliance with the European Convention on Animal Care. All experimental procedures and protocols used in this investigation were reviewed and approved by the Ethical Committee of the Medical Faculty of the University of Liege.

All animals were premedicated with intramuscular administration of ketamine (20 mg/kg) and diazepam (1 mg/kg). Anesthesia was then induced and maintained by a continuous infusion of sufentanil (0.5 µg kg^{-1} h^{-1}) and sodium pentobarbital (3 mg kg^{-1} h^{-1}). Spontaneous movements were prevented by pancuronium bromide (0.1 mg/kg). After endotracheal intubation through a cervical tracheostomy, the pigs were connected to a volume-cycled ventilator (Evita 2, Dräger, Lübeck, Germany) set to deliver a tidal volume of 10 ml/kg at a respiratory rate of 20/min. End-tidal CO_2 measurements (Capnomac, Datex, Helsinki, Finland) were used to monitor the adequacy of ventilation. Respiratory settings were adjusted to maintain end-tidal CO_2 between 30 and 35 mmHg. Arterial oxygen saturation was monitored closely and maintained above 95% by adjusting the F_IO_2 as necessary. Temperature was maintained at 37 °C by means of a heating blanket. A standard lead electrocardiogram was used for the monitoring of heart rate (HR).

The chest was opened with a mid-sternotomy, the pericardium was incised and sutured to the chest wall to form a cradle for the heart, and the root of the aorta was dissected clear of adherent fat and connective tissue. A 7-F, 12-electrode (8-mm interelectrode distance) conductance micromanometer-tipped catheter (CD Leycom, Zoetermeer, The Netherlands) was inserted through the right carotid artery and advanced into the left ventricle. A micromanometer-tipped catheter (Sentron pressure measuring catheter, Cordis, Miami, FL, USA) was inserted through the right femoral artery and advanced into the ascending aorta. A 14-mm diameter perivascular flow probe (Transonic Systems Inc., Ithaca, NY, USA) was closely adjusted around the aorta 2 cm downstream to the aortic valve. The micromanometer-tipped catheter was manipulated so that the pressure sensor was positioned just distal to the flow probe. Also, a second micromanometer-tipped catheter was advanced in the descending thoracic aorta through the left femoral artery, for measurement of distal aortic pressure. Right atrial pressure was measured with a micromanometer-tipped catheter inserted into the cavity through the superior vena cava. A 6-F Fogarty balloon catheter (Baxter Healthcare Corp., Oakland, CA, USA) was advanced into the inferior vena cava through a right femoral venotomy. Inflation of this balloon produced a gradual leftward shift in pressure-volume loops by reducing venous return. Thrombus formation along the catheters was prevented by administration of 100 U/kg of heparin sodium intravenously just before the insertion. The surgical preparation is illustrated in Fig. 1.

2.2. Experimental protocol

In order to provide similar states of vascular filling, the animals were continuously infused with Ringer lactate (5 ml kg^{-1} h^{-1}), and, when necessary, with hydroxyethylstarch 6% to increase central venous pressure up to 6-7 mmHg over 30 min. Baseline hemodynamic recording was obtained thereafter from simultaneous measurements of aortic pressure and flow waves necessary to identify the four-element windkessel model parameters (Fig. 2). A first diagram of LV pressure-volume relationship was generated from volume and pressure measurements at baseline and after stepwise decreases in preload by reducing venous return. The occlusion was limited to a few seconds in duration in order to avoid reflex responses. All measurements were taken immediately after the animal was briefly disconnected from the ventilator to sustain end-expiration. After deflation of the inferior vena cava balloon, the animals were allowed to rest for an additional 30 min.

Fig. 1: *Schematic diagram of the surgical preparation. (a) Left ventricular conductance micromanometer-tipped catheter. (b) Aortic micromanometer-tipped catheter. (c) Aortic flow probe. (d) Right atrial micromanometer-tipped catheter. (e) Inferior vena cava Fogarty balloon catheter. (f) Aortic banding. The micromanometer-tipped catheter placed in the descending thoracic aorta is not shown in this figure.*

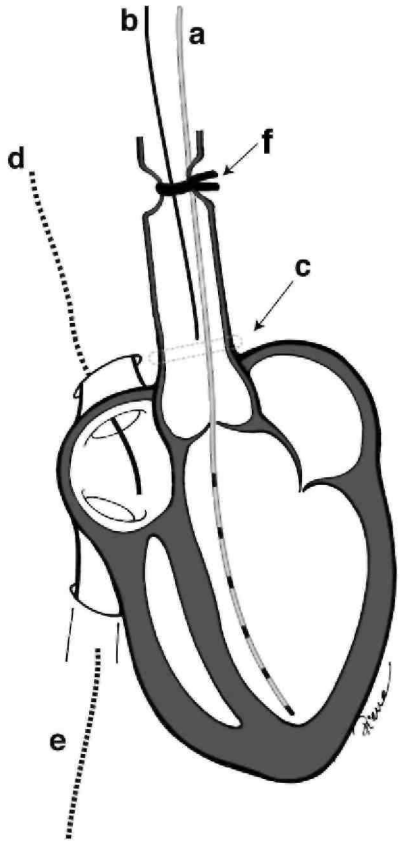

Fig. 2: *Electric analogue of the four-element windkessel model. R_1; characteristic impedance; R_2, peripheral resistance; C, compliance; L, inductance.*

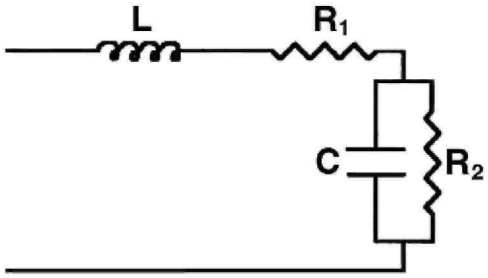

In each group, after hemodynamic measures at baseline (Basal), left ventricular afterload was increased by tightening a narrow band transversally around the ascending thoracic aorta, before the origin of the brachiocephalic artery. The band was tightened so that the systolic aortic pressure was increased by 20% (Fig. 1). Hemodynamic measurements were repeated after the aortic banding had been in place for 30 min (Band).

After this second set of hemodynamic measures, aortic banding was removed. After 30 min of rest, hemodynamic measurements were obtained (Basal 2).

The autonomic nervous system was then inhibited by atropine sulfate (intravenous injection of 0.2 mg/kg, followed by infusion at 1 mg kg^{-1} h^{-1}) and hexamethonium chloride (intravenous injection of 6 mg/kg, followed by infusion at 3 mg kg^{-1} h^{-1}). When mean aortic pressure and HR were stabilized, another set of hemodynamic measures was obtained (Hexa).

Finally, the aortic banding was then reinstalled and, after another resting period of 30 min, the measurements were repeated (Band Hexa). Care was taken as to always reinstall the banding at the same location on the ascending aorta in both experimental situations. Furthermore, a mark was drawn on the banding to ensure the exact same degree of constriction, with and without autonomous system blockade.

For each animal, three sets of measures were obtained at each state. Blood samples were collected for hematocrit measurements at Basal, Band and Band Hexa states.

2.3. Data collection

The conductance catheter was connected to a Sigma-5 signal-conditioner processor (CD Leycom, Zoetermeer, The Netherlands). The ultrasonic flow probe was connected to a flow-meter (HT 207, Transonic Systems Inc., Ithaca, NY, USA), and each micromanometer-tipped catheter to the appropriate monitor (Sentron pressure monitoring, Cordis, Miami, FL, USA).

All analog signals and ventricular pressure-volume loops were displayed on screen for continuous monitoring. The analog signals were continuously converted to digital form with an appropriate software (Codas, DataQ Instruments Inc., Akron, OH, USA) at a sampling frequency of 200 Hz.

2.4. Data analysis

2.4.1. Ventricular systolic function

Left ventricular volumes were inferred using the dual field conductance catheter technique [3,4]. Calibration of the conductance signal to obtain absolute volume was performed by the hypertonic saline method [3]. Therefore, a small volume (1-2 ml) of 10% NaCl solution was injected into the pulmonary artery during continuous data acquisition.

2.4.2. LV contractile function was assessed by the end-systolic pressure-volume relation (ESPVR), and the stroke work (SW)

The instantaneous pressure-volume relationship was considered in terms of a time-varying elastance *E(t)*, defined by the following relationship:

$$E(t) = P(t)/[V(t) - Vd]$$

where *P(t)* and *V(t)* are respectively the instantaneous ventricular pressure and volume, and V_d a correction term. End-systole was defined as the instant of time in the ejection phase at which *E(t)* reaches its maximum, E_{max}[3]. It is has been demonstrated that *E(t)* and V_d are insensitive to preload, at least within physiological ranges. Preload was acutely reduced by inflating the inferior vena cava balloon catheter. Stroke work (SW) was the integrated area of each PV loop.

2.4.3. Myocardial energetics

Myocardial energetics was assessed by computation of pressure-volume area (PVA). In the time-varying elastance model of the ventricle, the total energy generated by each contraction is represented by the total area under the end-systolic pressure-volume relation line and the systolic segment of the pressure-volume loop, and above the end-diastolic pressure volume relation curve, and denoted by PVA (Fig. 3) [5]. PVA is the sum of SW, or the energy that the ventricle delivers to the blood at ejection, and potential energy (PE), necessary to overcome the viscoelastic properties of the myocardium itself. It has been demonstrated that PVA was highly correlated with myocardial oxygen consumption [6].

Mechanical efficiency was defined as the SW/PVA ratio.

2.4.4. Arterial properties

Arterial properties were assessed from ascending aortic pressure and flow measurements and represented with a four-element windkessel model (WK4) [7]. An electrical analog of the WK4 is displayed in Fig. 2. In this model, the resistor R_2 represents the resistive properties of the systemic bed, which are considered to reside primarily in

the arteriolar system. The capacitor C, placed in parallel with R_2, represents the compliant properties of the systemic vessels. The resistor R_1 represents the characteristic impedance, which level depends prominently on the elastic properties of the aorta. Finally, an inductance, L, is introduced to take blood inertia into account. Furthermore, L restores positive phase angles at high frequencies of the impedance spectrum [8].

Fig. 3: *Pressure-volume area (PVA). P_v, ventricular pressure; V_v, ventricular volume; SW, stroke work; PE, potential energy; PVA, SW + PE.*

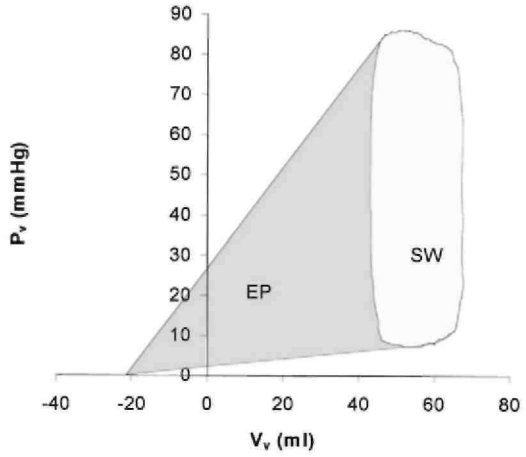

The values of R_1 R_2, C, and L were estimated by a method previously described [9].

Effective arterial elastance (E_a) was calculated according to the equation [10]:

$$E_a = \frac{R_1 + R_2}{T_s + R_2 C\left(1 - e^{-R_2 C/T_d}\right)}$$

where T_s and T_d are the systolic and diastolic time intervals, respectively. T_s was calculated in the aortic pressure wave, as the time interval between the point just before the abrupt rise and the dicrotic notch.

Ventriculo-arterial coupling was appreciated through the ratio E_{es}/E_a.

2.5. Statistical analysis

Data are expressed as mean ± standard error of the mean (S.E.M.).

Statistical comparison of data during the different experimental conditions was conducted by a two-way analysis of variance for repeated measurements with experimental condition and pig as factors, followed by Scheffe's multiple comparisons test if the analysis of variance resulted in a P value <0.05.

Results of statistical tests were considered significant for a level of uncertainty of 5% ($P < 0.05$). Statistical tests were performed using Statistica software (Statsoft Inc., Tulsa, OK, USA).

3. Results

3.1. Effects of aortic banding, with and without autonomic blockade, on conventional hemodynamic parameters

As shown in Table 1, increased LV afterload by proximal aortic banding induced a significant ($P < 0.001$) increase in systolic proximal aortic pressure, while diastolic proximal aortic pressure remained constant. When the autonomic nervous system was inhibited, variations of proximal aortic pressure were of the same magnitude as those observed when the baroreflex was intact. In addition, after proximal aortic banding, distal aortic pressure decreased similarly in both conditions ($P < 0.01$).

After aortic banding, mean cardiac output slightly but significantly ($P < 0.05$) decreased, while HR increased (P

< 0.001). After autonomic blockade and aortic banding, cardiac output decreased significantly ($P < 0.001$), while HR remained constant (Table 1). Hematocrit was 52 ± 2% at baseline, 50 ± 3% at the end of aortic banding without autonomous blockade, and 51 ± 4% at the end of the experimental protocol (NS).

3.2. Effects of aortic banding, with and without autonomic blockade, on windkessel model parameters values

As shown in Table 2, after aortic banding (with and without autonomic blockade), R_1 and L increased, while C decreased. However, after aortic banding alone, R_2 increased significantly while, after aortic banding and autonomic blockade, R_2 decreased significantly ($P < 0.001$). Integrating these parameters, E_a increased by 36% ($P < 0.001$) after aortic banding with intact baroreflex and by 13% after aortic banding and autonomic blockade. Such a difference between the two experimental conditions was significant ($P < 0.01$).

Table 1: *Effect of aortic banding with and without autonomic blockade on conventional hemodynamic parameters*

	Basal	**Band**	**Basal 2**	**Hexa**	**Band Hexa**
P_{sys} **(mmHg)**	96 ± 6	119 ±3*	96 ±4	95 ± 5	123 ± 3$^{\#}$
P_{dia} **(mmHg)**	56 ±4	56 ±2	57 ± 3	61 ± 2	62 ±4
P_{desc} **(mmHg)**	74 ± 5	62 ±6*	72 ± 5	73 ± 6	60 ±5$^{\#}$
CO (ml/s)	53 ± 3	49 ± 2*	52 ±4	52 ± 3	46 ± 3$^{\#}$
HR (beats/min)	115 ± 5	125 ± 2*	117 ±4	119 ±4	121 ± 3

P_{sys}, systolic aortic pressure; P_{dia}, diastolic aortic pressure; P_{desc}, mean descending aortic pressure; CO, cardiac output; HR, heart rate. *$P < 0.05$ vs. basal; $^{\#}P < 0.05$ vs. Hexa; $^{\S}P < 0.05$ vs. Band.

Table 2: *Effect of aortic banding with and without autonomic blockade on windkessel model parameters*

	Basal	**Band**	**Basal 2**	**Hexa**	**Band Hexa**
R_1 **(mmHg.s/ml)**	0.13 ± 0.01	0.35 ± 0.01*	0.14 ± 0.01	0.16 ± 0.01	0.37 ± 0.01$^{\#}$
R_2 **(mmHg.s/ml)**	1.5 ± 0.1	1.7 ± 0.1*	1.5 ±0.1	1.6 ±0.1	1.4 ± 0.1$^{\#}$
C (ml/mmHg)	0.57 ± 0.04	0.41 ± 0.05*	0.54 ± 0.07	0.53 ± 0.06	0.39 ± 0.05$^{\#}$
L **(mmHg.s^2 /ml)**	0.002 ± 0.0003	0.004 ± 0.0003*	0.002 ± 0.0002	0.002 ± 0.0003	0.004 ± 0.0004$^{\#}$
E_a **(mmHg/ml)**	3.4 ± 0.3	4.6 ± 0.2*	3.4 ± 0.3	3.6 ± 0.3	4.1 ± 0.3$^{\#\S}$

R_1, characteristic impedance; R_2, peripheral resistance; C, compliance; L, inductance; E_a, effective arterial elastance. *$P < 0.05$ vs. basal; $^{\#}P < 0.05$ vs. Hexa; $^{\S}P < 0.05$ vs. Band.

3.3. Effects of aortic banding, with and without autonomic blockade, on left ventricular volumes and pressures

Aortic banding increased significantly ($P < 0.001$) end-systolic volume, while end-diastolic volume was unchanged (Table 3). Therefore, stroke volume and ejection fraction significantly ($P < 0.001$) decreased (Table 3). Aortic banding after autonomic blockade also induced a significant ($P < 0.001$) increase in end-systolic volume, at constant end-diastolic volume. Therefore, stroke volume and ejection fraction significantly ($P < 0.001$) decreased. However, all these variations were significantly ($P < 0.01$) more severe than those observed with an intact baroreflex.

Evolution in ventricular pressures was of the same magnitude after aortic banding with or without autonomic blockade (Table 3).

3.4. Effects of aortic banding, with and without autonomic blockade, on left ventricular function

As shown in Table 4 and Fig. 4, after aortic banding, E_{es} increased by 31% ($P < 0.001$) and V_d decreased from -3.6 ± 0.2 to -6.8 ± 0.3 ml ($P = 0.001$). As a consequence, E_{es}/E_a remained stable and close to the optimal value. After aortic banding and autonomic blockade, E_{es} increased by 15% ($P < 0.01$), V_d decreased significantly ($P = 0.01$), and E_{es}/E_a remained stable.

Table 3: *Effect of aortic banding with and without autonomic blockade on left ventricular volumes and pressures*

	Basal	Band	Basal 2	Hexa	Band Hexa
EDV (ml)	49 ±4	50 ± 5	50 ±3	51 ±4	53 ±4
ESV (ml)[a]	28 ± 3	33 ± 2*	29 ± 2	33 ± 3	43 ± 3$^{\#\S}$
SV (ml)	27 ± 2	24 ± 1	26 ± 2	25 ± 2	20 ± 1
EF (%)	54 ±2	48 ± 3*	52 ±2	50 ± 2	38 ± 2$^{\#\S}$
P_{es} (mmHg)	94 ±7	116 ±4*	92 ±5	90 ± 6	122 ± 5$^{\#}$
P_{ed} (mmHg)	5 ± 1	4 ± 1	4 ± 1	5 ± 1	6 ± 1

EDV, end-diastolic volume; ESV, end-systolic volume; SV, stroke volume; EF, ejection fraction; P_{es}, end-systolic pressure; P_{ed}, end-diastolic pressure. *$P < 0.05$ vs. basal; $^{\#}P < 0.05$ vs. Hexa; $^{\S}P < 0.05$ vs. Band.

[a] ESV is the volume measured at the time of maximal end-systolic elastance; it is therefore different from end-ejection volume.

Aortic banding increased SW by 44% *(*$P < 0.005$) and PVA by 57% *(*$P < 0.001$). Therefore, mechanical efficiency SW/PVA significantly decreased *(*$P < 0.01$). After autonomic blockade, aortic banding also increased SW by 43% *(*$P < 0.005$) and PVA by 63% *(*$P < 0.001$) while mechanical efficiency SW/PVA significantly *(*$P < 0.01$) decreased. Autonomic blockade did not modify the evolution of these parameters after aortic banding.

4. Discussion

The effect of aortic banding on the mechanical properties of the proximal aorta is expressed by an increase in R_1 and a decrease in *C*. The reduction of the internal vascular diameter increases wave reflections, thereby increasing *L*. These mechanical effects of the aortic banding are unaffected by autonomic nervous system inhibition.

In the intact cardio-vascular system, the systemic pressure drop distal to the aortic banding is perceived by the baroreceptors, mainly located in the transverse aortic and carotid arteries wall. This results in a stimulation of the baroreflex, with increase in R_2 as a vascular effect. The significant increase in HR that we observe can also be interpreted as an expression of baroreflex stimulation.

On the opposite, when the autonomic nervous system is inhibited, the decrease in systemic pressure, distal to the aortic banding, is not associated with peripheral vasoconstriction. In addition, under these circumstances, HR remains constant.

These changes in the parameters characterizing the systemic vasculature are responsible for a significant increase in E_a, which is of a greater magnitude when the autonomic nervous system remains intact.

This afterload increase is associated with an augmentation of LV performance, as demonstrated by increased E_{es} and SW, at constant end-diastolic volume, and by ESPVR leftward shift (decrease of V_d). Therefore, E_{es}/E_a remains close to baseline value. This augmentation of LV performance is unaffected by the inhibition of the baroreflex.

Table 4: *Effect of aortic banding with and without autonomic blockade on left ventricular function*

	Basal	Band	Basal 2	Hexa	Band Hexa
E_{es} (mmHg/ml)	2.81 ±0.18	3.69 ± 0.2*	2.74 ± 0.24	2.92 ± 0.19	3.34 ± 0.16$^{\#}$
V_d (ml)	-3.6 ±0.2	-6.8 ±0.3*	-2.3 ± 0.2	- 1 ± 0.4	-4.6 ± 0.6$^{\#}$
E_{es}/E_a	0.84 ± 0.14	0.81 ±0.11	0.80 ± 0.12	0.80 ± 0.13	0.81 ± 0.15
SW (mmHg.ml)	2012 ± 168	2912 ± 114*	2119 ± 124	1948 ± 158	2786 ± 142$^{\#}$
SW/PVA	0.7 ± 0.1	0.6 ± 0.1*	0.7 ± 0.1	0.7 ± 0.1	0.6 ± 0.1$^{\#}$

E_{es}, end-systolic elastance; V_d, dead volume; E_{es}/E_a, systemic ventriculo-arterial coupling; SW, stroke work; SW/PVA, mechanical efficiency. *$P < 0.05$ vs. basal; $^{\#}P < 0.05$ vs. Hexa; $^{\S}P < 0.05$ vs. Band.

Several experimental studies have evaluated the effect of afterload on LV performance, in isolated heart preparations and on intact animals. The results were contradictory.

Indeed, Sunagawa et al. [1] and Freeman [11] have observed that afterload augmentation induced a leftward shift

of ESPVR, without changing E_{es}.

On the opposite, Baan and Enno [12] and Asanoi et al. [13] have found that the increase in E_a was associated with an augmentation of E_{es}, in addition to ESPVR leftward shift. All these experiments were conducted under autonomic nervous system inhibition. However, it should be emphasized that Asanoi et al. [13] obtained an afterload increase by infusing angiotensin II, a substance with powerful vasoconstrictive properties, but which can also directly affect myocardial contractility.

Several studies [14,15] also investigated the influence of autonomic nervous system on ESPVR and found results that were substantially similar to ours. Assessing the determinants of ESPVR during acute regional ischemia in open-chest dogs, Kass et al. [14] showed that the amount of rightward shift and the decrease in the slope of ESPVR were independent of baroreflex integrity. In another study performed on open-chest dogs, Schipper et al. [15] demonstrated that cardiac sympathetic denervation did not change the load dependence of ESPVR.

Fig. 4: *Typical pressure-volume loops recordings at baseline (A and C) and during aortic banding (B and D), with (C and D) and without autonomous nervous system blockade (A and B).*

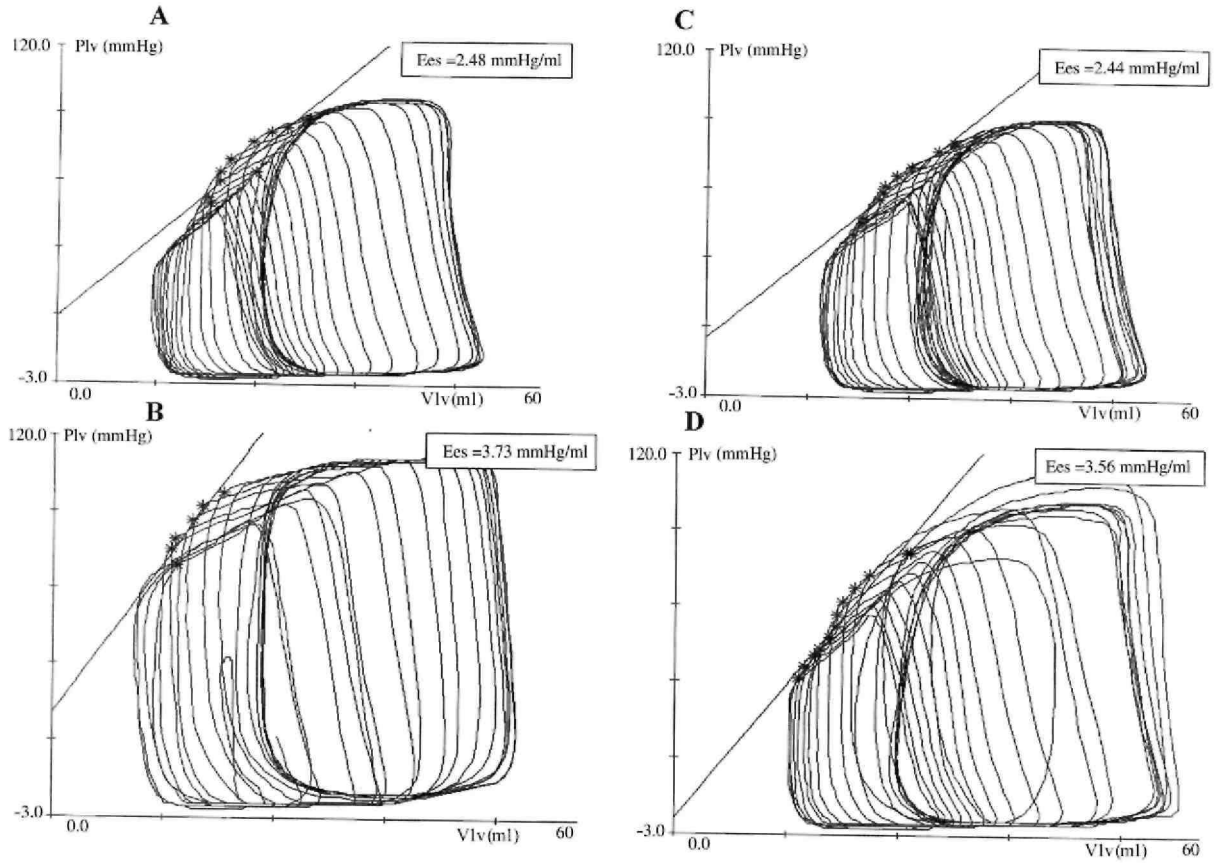

A too strict interpretation of the changes in ESPVR would conclude that a leftward shift, without slope variations, reflects that an afterload augmentation is not associated with an increase in myocardial contractility per se. However, as correctly emphasized by Sagawa et al. [10], the controversy regarding the interpretation of ESPVR should prevent the use of isolated slope or volume intercept values to characterize the contractile state. Since in all of these studies, the end-systolic point under afterload augmentation is always to the left of the control point in the pressure-volume plane, LV performance always appears increased.

In our study, while afterload augmentation is accompanied by an increase in LV performance, we observe a decrease in the efficiency of the energetic transfer from PVA to external mechanical work. This alteration in mechanical efficiency is independent of baroreflex integrity. Our results are in accordance with similar observations on anesthetized close-chest dogs [11,16].

What are the mechanisms that could explain such an augmentation of LV performance in the face of increased

afterload?

Studies on isolated heart preparations [17] and in situ [18,19] have shown LV performance to be increased at longer end-diastolic ventricular length, probably due to increased myofiber sensitivity to calcium. However, in our study, the augmentation of LV performance in the face of increased afterload is observed at matched end-diastolic volumes. Therefore, the mechanism of length-dependant activation is unlikely to play a significant role in our observations.

Our results support the theory of homeometric auto-regulation, which was described by Sarnoff et al. [20]on an isolated heart preparation. The homeometric autoregulation suggests a mechanism by which the heart can maintain a constant stroke volume in the face of increased afterload, without using the Starling mechanism. It has been suggested that homeometric regulation is explained by an increased coronary perfusion secondary to the increased aortic pressure. Indeed, Abel et al. demonstrated that increased coronary perfusion results in an improvement of the contractile performance of the left ventricle [21].

Another potential explanation for the improved LV contractile performance lies on increased wall tension. Effectively, increased end-systolic pressure could act on mechanical stretch-activated channels. Deformation of the cell membrane by increase in transmembrane pressure gradient could be sufficient to increase calcium release from the endoplasmic reticulum [22]. Another endogenous stimulus for adjustment of contractile performance could originate from the endocardial endothelium, which acts as a sensing system and plays an obligatory role in regulating cardiac function [23].

There are several possible to our study. First, our experimental protocol take some time (about 2 h from the basal measurements), and to ensure equal volumes by infusion to a certain central venous pressure could cause a considerable hemodilution which in itself would influence the resting cardiovascular state. At the same time, a substantial amount of blood loss could occur because the pigs are partially heparinized. However, our hematocrit measurements rule out such an experimental limitation.

Second, we lack one control group, which is to follow pigs over time with the same interventions, but without autonomic blockade. If there is a change in the cardiovascular status of the pigs throughout the experiment, then we cannot really rely on the animals as their own control. However, our hemodynamic results show that the experimental preparation is very stable. Furthermore, we have recently published the data from a different protocol (ischemia preparation), including a true control group with sham-operated animals, showing no significant hemodynamic changes over 6 h [24].

Our data confirm the results of Schipper et al. who demonstrated that improved LV contractile performance in response to an increased afterload is not abolished by sympathetic and parasympathetic denervation [15]. Such mechanisms of autoregulation, independent of the autonomic nervous system, are of paramount importance in heart transplant patients. Indeed, such patients, although lacking cardiac innervation, can adapt their cardiac output, stroke volume, end-systolic and end-diastolic pressures without simultaneous changes in heart rate.

In conclusion, our results demonstrate that an increase in LV afterload has a composite effect on LV function. Ventricular performance is increased, as expressed by ESPVR leftward shift, increase in E_{es} and SW but mechanical efficiency is decreased. These changes are observed independently of baroreflex integrity.

Acknowledgements

This work was supported by grants from the ARC 94/99-177 of the Communauté Française de Belgique, from the Belgian National Fund for Scientific Research, and from the Leon Fredericq Foundation of the University of Liege. Vincent Tchana-Sato is funded by a doctoral grant of the National Fund for Scientific Research, Belgium, and Philippe Kolh is partially funded by a post-doctoral grant of the National Fund for Scientific Research, Belgium.

References

[1] Sunagawa K, Maughan WL, Sagawa K. Stroke volume effect of changing arterial input impedance over selected frequency ranges. Am J Physiol 1985;248(4 Pt. 2):H477-84.

[2] Ross JJ. Afterload mismatch and preload reserve: a conceptual framework for the analysis of ventricular function. Prog Cardiovasc Dis 1976;18:255-64.

[3] Suga H, Kitabatake A, Sagawa K. End-systolic pressure determines stroke volume from fixed end-diastolic volume in the isolated canine left ventricle under a constant contractile state. Circ Res 1979;44: 238-49.

[4] Steendijk P, van der Velde ET, Baan J. Left ventricular stroke volume by single and dual excitation of conductance catheter in dogs. Am J Physiol 1993;264:H2198-207.

[5] Suga H. Total mechanical energy of a ventricle model and cardiac oxygen consumption. Am J Physiol 1979;236:H498-H505.

[6] Denslow S. Relationship between PVA and myocardial oxygen consumption can be derived from thermodynamics. Am J Physiol 1996;270:H730-40.

[7] Westerhof N, Elzinga G, Sipkema P. An artificial arterial system for pumping hearts. J Appl Physiol 1971;31:776-81.

[8] Grant BJ, Paradowski LJ. Characterization of pulmonary arterial input impedance with lumped parameter models. Am J Physiol 1987;252(3 Pt. 2):H585-93.

[9] Lambermont B, Kolh P, Detry O, Gerard P, Marcelle R, D'Orio V. Analysis of endotoxin effects on the intact pulmonary circulation. Cardiovasc Res 1999;41(1):275-81.

[10] Sagawa K, Maughan L, Suga H, Sunagawa K. Cardiac contraction and the pressure-volume relationship. New York: Oxford University Press; 1988.

[11] Freeman GL. Effects of increased afterload on left ventricular function in closed-chest dogs. Am J Physiol 1990;259(2 Pt. 2): H619-25.

[12] Baan J, Enno T. Ventricular pressure-volume relations demonstrate positive inotropic effect of increased arterial impedance. In: Hori M, Suga H, Baan J, Yellin EL, editors. Cardiac mechanics and function in the normal and diseased heart. Tokyo, Japan: Springer-Verlag; 1989. p. 189-97.

[13] Asanoi H, Ishizaka S, Kameyama T, Sasayama S. Neural modulation of ventriculoarterial coupling in conscious dogs. Am J Physiol 1994; 266(2 Pt. 2):H741-8.

[14] Kass DA, Marino P, Maughan W, Sagawa K. Determinants of end-systolic pressure-volume relations during acute regional ischemia in situ. Circulation 1989;80:1783-94.

[15] Schipper IB, Steendijk P, Klautz RJ, van der Velde ET, Baan J. Cardiac sympathetic denervation does not change the load dependence of the left ventricular end-systolic pressure/volume relationship in dogs. Pflugers Arch Eur J Physiol 1993;425(5-6): 426-33.

[16] Nozawa T, Yasumura Y, Futaki S, Tanaka N, Uenishi M, Suga H. Efficiency of energy transfer from pressure-volume area to external mechanical work increases with contractile state and decreases with afterload in the left ventricle of the anesthetized closed-chest dog. Circulation 1988;77(5): 1116-24.

[17] Lakatta E, Jewell B. Length-dependant activation ; its effects on the length-tension relation in cat ventricular muscle. Circ Res 1977;40:251-7.

[18] Little W. The left ventricular DP/Dtmax—end-diastolic volume relation in closed-chest dogs. Circ Res 1985;56:808-15.

[19] Sugiura S, Hunter WC, Sagawa K. Long-term versus intrabeat history of ejection as determinants of canine ventricular end-systolic pressure. Circ Res 1989;64:255-64.

[20] Sarnoff SJ, Mitchell JH, Gilmore MS, Remensnyder JP. Homeometric autoregulation in the heart. Circ Res 1960;8:1077-91.

[21] Abel RM, Reis RL. Effects of coronary blood flow and perfusion pressure on left ventricular contractility in dogs. Circ Res 1970;27(6):961-71.

[22] Morris CE. Mechanosensitive ion channels. J Membr Biol 1990; 113(2):93-107.

[23] Brutsaert DL, Fransen P, Andries LJ, De Keulenaer GW, Sys SU. Cardiac endothelium and myocardial function. Cardiovasc Res 1998; 38(2):281-90.

[24] Rolin S, Petein M, Tchana-Sato V, Dogne JM, Benoit P, Lambermont B, Ghuysen A, Kolh P, Masereel B. BM-573, a dual thromboxane synthase inhibitor and thromboxane receptor antagonist, prevents pig myocardial infarction induced by coronary thrombosis. J Pharmacol Exp Ther 2003;306(l):59-65.